Neurotherapeutics (2019) 16:523–537
https://doi.org/10.1007/s13311-019-00711-w

ORIGINAL ARTICLE

Anti-Inflammatory and Neuroprotective Effects of DIPOPA (N,N-Diisopropyl-2-Oxopropanamide), an Ethyl Pyruvate Bioisoster, in the Postischemic Brain

Hye-Kyung Lee[1,2] · Ju-Young Park[3] · Hahnbie Lee[1,2] · Il-Doo Kim[1,4] · Seung-Woo Kim[2,4] · Sung-Hwa Yoon[3] · Ja-Kyeong Lee[1,2]

Published online: 24 January 2019
© The American Society for Experimental NeuroTherapeutics, Inc. 2019

Abstract

Ethyl pyruvate (EP) is a simple aliphatic ester of pyruvic acid and has been shown to have protective properties, which have been attributed to its anti-inflammatory, anti-oxidative, and anti-apoptotic functions. In an effort to develop better derivatives of EP, we previously synthesized DEOPA (N,N-diethyl-2-oxopropanamide, a novel isoster of EP) which has greater neuroprotective effects than EP, probably due to its anti-inflammatory and anti-excitotoxic effects. In the present study, we synthesized 3 DEOPA derivatives, in which its diethylamino group was substituted with diisopropylamino, dipropylamino, or diisobutylamino groups. Among them, DIPOPA (N,N-diisopropyl-2-oxopropanamide) containing diisopropylamino group had a greater neuroprotective effect than DEOPA or EP when administered intravenously to a rat middle cerebral artery occlusion (MCAO) model at 9 h after MCAO. Furthermore, DIPOPA had a wider therapeutic window than DEOPA and a marked reduction of infarct volume was accompanied by greater neurological and behavioral improvements. In particular, DIPOPA exerted robust anti-inflammatory effects, as evidenced by marked suppressions of microglia activation and neutrophil infiltration in the MCAO model, in microglial cells, and in neutrophil–endothelial cocultures at lower concentration, and did so more effectively than DEOPA. In particular, DIPOPA remarkably suppressed neutrophil infiltration into brain parenchyma, and this effect was attributed to the expressional inhibitions of cell adhesion molecules in neutrophils of brain parenchyma and in circulating neutrophils via NF-κB inhibition. Together, these results indicate the robust neuroprotective effects of DIPOPA are attributable to its anti-inflammatory effects and suggest that DIPOPA offers a potential therapeutic means of ameliorating cerebral ischemic injury and other inflammation-related pathologies.

Key Words DIPOPA · Stroke · Anti-inflammation · Ethyl pyruvate · NF-κB

Introduction

Ethyl pyruvate (EP) is a simple aliphatic ester of pyruvate and has been shown to ameliorate injuries in various disease models. For example, EP has been reported to reduce mortality in lethal models of hemorrhagic shock and sepsis [1, 2], to significantly mitigate acute pancreatitis-induced damage [3], and to reduce infarct volumes and improve motor function scores in an animal model of ischemic stroke [4]. The protective effects of EP have been reported to be due to its anti-inflammatory, anti-oxidative, anti-apoptotic, and ion-chelating effects [5–8]. Various molecular mechanisms have been proposed to explain its anti-inflammatory effects. Han et al. [9] reported EP suppresses the DNA binding of p65 (a NF-κB subunit) by oxidizing its cysteine residue, and by doing so inhibits the inductions of inflammatory cytokines

Hye-Kyung Lee and Ju-Young Park contributed equally to this work.

✉ Sung-Hwa Yoon
shyoon@ajou.ac.kr

✉ Ja-Kyeong Lee
jklee@inha.ac.kr

[1] Department of Anatomy, Inha University School of Medicine, Michuhol-gu Inharo 100, Inchon 22202, Republic of Korea

[2] Medical Research Center, Inha University School of Medicine, Michuhol-gu Inharo 100, Inchon 22202, Republic of Korea

[3] Department of Molecular Science and Technology, Ajou University School of Medicine, Suwon, Republic of Korea

[4] Department of Biomedical Sciences, Inha University School of Medicine, Inchon, South Korea

regulated by NF-κB. EP was also reported to suppress the secretion/release of high mobility group box-1 (HMGB1; a danger-associated molecular pattern molecule) [8, 10, 11]. Interestingly, Han et al. [9] reported that the anti-inflammatory effect of EP is related to its anti-oxidative effect and, in a previous study, we also showed the interrelationship between these 2 effects in BV2 cells, in that EP mediated the nuclear translocation of Nrf2 and Nrf2 competed with p65 for p300 binding [12]. Regarding the ion-chelating effects of EP, we found the neuroprotective effect of EP due, at least in part, to its ability to protect cells from toxic effects of Zn^{2+} via a direct chelation of Zn^{2+} and the inhibition of NAD depletion [13].

Based on the reported beneficial effects of EP, many researchers have screened derivatives of EP or modified the chemical structure of EP to fortify its therapeutic effects. Sappington et al. [14] showed that diethyl oxaloproprionate (DEOP) and 2-acetamidoacrylate (2AA) (both commercially available EP analogues) have anti-inflammatory and cytoprotective properties, and found that the methyl ester of 2-acetamidoacrylate (methyl-2-acetamidoacrylate, Me-2AA) had greater anti-inflammatory effects than 2AA or EP. Min et al. [15] reported EOP (S-ethyl oxopropanethioate) had anti-inflammatory effects in LPS-treated BV2 cells, but later, we found it had no meaningful neuroprotective effect in the postischemic brain [16]. Furthermore, in the same study, we generated novel EP isosteres, and of these, DEOPA (N,N-diethyl-2-oxopropanamide), which contains a diethylamino group instead of the ethoxy group of EP, displayed greater neuroprotective, anti-inflammatory, and anti-excitotoxic effects than EP in the postischemic brain [16].

In an effort to develop a more effective therapeutic agent based on DEOPA, we synthesized 3 derivatives of DEOPA by replacing its diethyl group with a dipropyl, diisopropyl, or diisobutyl group. The neuroprotective effects of these derivatives were examined in a rat middle cerebral artery occlusion (MCAO) model of stroke, and the molecular mechanisms responsible were investigated in microglia, neutrophil, neutrophil–endothelial cell coculture, and primary cortical neuron cultures.

Materials and Methods

General Procedure for the Synthesis of the 3 DEOPA Analogues

2-Oxopropanoyl chloride (**2**) (1 equivalent), which was prepared from pyruvic acid (**1**) and α,α-dichloromethyl methyl ether, was added to a solution of the corresponding amines (3 equivalent) and triethylamine (3 equivalent) in dichloromethane at 0 °C. The mixtures were stirred at room temperature for 4 h and then quenched with 1 *N* HCl solution. The solutions were extracted with ethyl acetate, and organic layers were washed with water and brine, dried over Na_2SO_4, and evaporated *in vacuo*. The crude residues were purified by silica column chromatography to give the title compounds (**3a**-**3c**).

2-Oxo-*N,N*-Dipropylpropanamide (3a)

The title compound was obtained as a yellow oil. ^{1}H NMR ($CDCl_3$) δ 0.85-0.90 (t, 3H, *J*= *7.6* Hz), 0.90-1.00 (t, 3H, *J*= *7.6* Hz), 1.55-1.70 (m, 4H), 2.41 (s, 3H), 3.15-3.23 (t, 2H, *J*= *7.6* Hz), 3.30-3.38 (t, 2H, *J*= *7.6* Hz); ^{13}C NMR ($CDCl_3$) δ 10.84, 11.11, 20.03, 21.97, 27.55, 46.21, 48.92, 166.57, 198.15.

N,N-Diisopropyl-2-Oxopropanamide (3b)

The title compound was obtained as a yellow oil. ^{1}H NMR ($CDCl_3$) δ 1.20-1.25 (d, 6H, *J*= *6.8* Hz), 1.40-1.48 (d, 6H, *J*= *6.4* Hz), 2.38 (s, 3H), 3.50-3.60 (q, 1H, *J*= *7.2* Hz), 3.70-3.80 (q, 1H, *J*= *6.4* Hz); ^{13}C NMR ($CDCl_3$) δ 20.19, 20.87, 27.39, 45.85, 49.68, 167.13, 198.44.

N,N-Diisobutyl-2-Oxopropanamide (3c)

The title compound was obtained as a yellow oil. ^{1}H NMR ($CDCl_3$) δ 0.76-0.85 (d, 6H, *J*= *6.8* Hz), 0.85-0.90 (d, 6H, *J*= *6.8* Hz), 1.74-1.88 (q, 1H, *J*= *6.4* Hz), 1.92-2.05 (q, 1H, *J*= *6.8* Hz), 2.34 (s, 3H), 3.00-3.10 (d, 2H, *J*= *7.6* Hz), 3.12-3.20 (d, 2H, *J*= *7.6* Hz);^{13}C NMR ($CDCl_3$) δ 19.81, 20.01, 26.23, 27.08, 27.84, 51.37, 54.51, 167.49, 198.17.

Intravenous Administrations of DEOPA Derivatives, DEOPA, or EP

DEOPA, DPOPA, or DIBOPA was dissolved in 0.01 M PBS and administered intravenously at 5 mg/kg body weight, and DIPOPA was administered intravenously at 1, 2, or 5 mg/kg body weight. EP was dissolved to a concentration of 28 mM in a solution containing Na^+ (130 mM), K^+ (4 mM), Ca^{2+} (2.7 mM), and Cl^- (139 mM) (pH 7.0) and also injected intravenously.

Surgical Procedure

Male Sprague Dawley rats (8-9 weeks old) were housed under diurnal lighting conditions and provided food and tap water *ad libitum*. All animal studies were carried out in strict ethical standards and they are specified in the Compliance with Ethical Standard section. MCAO was carried out as previously described [17]. In brief, the rats (250~300 g) were anesthetized with 5% isoflurane in a 30% oxygen/70% nitrous oxide gas mixture; anesthesia was maintained during procedures using 0.5% isoflurane

in the same gas mixture. The animals were randomly allocated to 10 treatment groups, as follows: 1) the MCAO group, PBS-treated MCAO animals ($n = 29$); 2) the MCAO + DIPOPA (N,N-diisopropyl-2-oxopropanamide) group, DIPOPA-treated MCAO animals ($n = 45$); 3) the MCAO + DPOPA (N,N-dipropyl-2-oxopropanamide) group, DPOPA-treated MCAO animals ($n = 5$); 4) the MCAO + DBIOPA (N,N-diisobutyl-2-oxopropanamide) group, DBIOPA-treated MCAO animals ($n = 4$); 5) the MCAO + DEOPA group, DEOPA-treated MCAO animals ($n = 32$); 6) the MCAO + EP group, EP-treated MCAO animals ($n = 34$); 7) the Sham group, the animals underwent surgery but were not subjected to MCAO ($n = 23$); 8) the sham + DIPOPA group, DIPOPA-treated sham control animals ($n = 5$); 9) the sham + DEOPA group, DEOPA-treated sham control animals ($n = 5$); or 10) the sham + EP group, EP-treated sham control animals ($n = 5$). MCAO was maintained for 1 h using a nylon suture and followed by reperfusion for up to 2 days. In each animal, the left femoral artery was cannulated for blood sampling to analyze pH, PaO_2, $PaCO_2$, and blood glucose concentrations (I-STAT; Sensor Devices, Waukesha, WI). Regional cerebral blood flow (rCBF) was monitored at 1 h post-MCAO using a laser Doppler flowmeter (Periflux System 5000; Perimed, Jarfalla, Sweden). A thermoregulated heating pad and a heating lamp were used to maintain a rectal temperature of 37.0 ± 0.5 °C during surgery. The mortality rate after operation was 5.1% (10/197). All measurements, including infarct volumes, neurological deficits, and latency in a rota-rod test, were conducted in a blind manner.

Infarct Volume Assessments

The rats were decapitated at 2 days post-MCAO, and whole brains were dissected coronally into 2-mm slices using a metallic brain matrix (RBM-40000, ASI, Springville, UT). The slices were immediately stained by immersing them in 2% TTC (2,3,5-triphenyl tetrazolium chloride) at 37 °C for 15 min and then fixed in 4% paraformaldehyde. Infarcted tissue areas were quantified using the Scion Image program (Frederick, MD). To avoid the distortion caused by edema and shrinkage, areas of ischemic lesions were calculated using the following equation: contralateral hemisphere volume − (ipsilateral hemisphere volume − measured injury volume) [18]. Infarct volumes were quantified (in mm^3) by multiplying summed section infarct areas by section thickness.

Modified Neurological Severity Scores

Neurological deficits were evaluated using modified neurological severity scores (mNSSs) at 2, 4, 6, 8, 10, 12, or 14 days post-MCAO. The mNSS system consists of motor, sensory, balance, and reflex tests, and overall results are graded using a scale of 0 to 18 (normal, 0; maximal deficit, 18) [19].

Rota-Rod Test

24 h before surgery, the rats were conditioned on a rota-rod unit at a constant speed (3 rpm) until they were able to remain on the rotating spindle for 180 s. At 2, 4, 6, 8, 10, 12, or 14 days post-MCAO, the rats were subjected to rota-rod testing at spindle speeds of 10 or 15 rpm and residence times on the spindle were recorded. A 1-h rest period was allowed between tests.

Immunohistochemistry

Immunological staining of brain sections was performed using a floating method, as previously described [20]. Primary antibodies were diluted as follows: 1:500 for anti-ionized calcium binding adaptor molecule-1 (Iba-1) (Wako Pure Chemicals, Osaka, Japan), 1:250 for anti-Mac2 (Abcam, Cambridge, UK), and 1:500 for anti-myeloperoxidase (MPO) (Abcam, Cambridge, UK). The experiments were repeated at least 3 times and representative images are presented.

Blood Neutrophil Isolation

Neutrophil was isolated from rat blood using Histopaque (Sigma-Aldrich, St. Louis, MO) gradients as previously described [21]. Briefly, Histopaque 1077 (3 ml) was layered on Histopaque 1119 (3 ml) in a 15-ml tube and rat blood (4 ml) was carefully placed on the top of the Histopaque mixture, which formed a 3-step gradient (Histopaque 1119/Histopaque1077/blood). The tube was then centrifuged at 400 × g for 30 min using a swinging rotor. The first ring, which contained mononuclear cells was slowly aspirated, and the second ring was transferred to another 15 ml tube containing PBS-BG (phosphate buffered solution, 0.1% bovine serum albumin, and 10% glucose) and centrifuged at 1500 g for 10 min. The pellet so obtained was suspended in 3 ml of PBS-BG, placed on Histopaque-1119 (3 ml), and centrifuged at 1500 g for 10 min at 4 °C. The ring that included neutrophils was then suspended in RPMI (Gibco BRL, Gaithersburg, MD) containing 1% FBS.

Cell Cultures

BV2 cells (a microglial cell line), human umbilical vein endothelial cells (HUVECs), and HL-60 cells (a human myelocytic leukemia cell line) were obtained from the American Type Culture Collection (ATCC, Rockville, MD). BV2 cells were

cultured as previously described [12]. HUVECs were cultivated in Endothelial Cell Medium (ScienCell, Corte Del Cedro, Carlsbad, CA), and HL-60 cells were cultivated in DMEM supplemented with 20% FBS and 100 U/ml penicillin/streptomycin. HL-60 differentiation was induced by treating cells with 1 μM all-trans retinoic acid (ATRA) (Sigma-Aldrich, St. Louis, MO) for 3 days. All cell lines were incubated at 37 °C in a humidified 95% air/5% CO_2 atmosphere.

Cell Viability Assay

Cell viability in BV2 cells (0.7×10^5) was measured using Cell Counting Kit-8 (Dojindo Molecular Technologies, Rockville, MD) by following the manufacturer's recommendation.

Nitrite Measurements

Nitrite production in BV2 cells (0.7×10^5) was measured as previously described [12].

RNA Preparation and RT-PCR

RNA was prepared using TRIzol reagent (Gibco BRL, Gaithersburg, MD). The sequences of the primers used for rat or mouse interleukin-6 (IL-6), rat tumor necrosis factor-α (TNF-α), rat interleukin-1β (IL-1β), rat inducible NO synthase (iNOS), mouse tumor necrosis factor-α (TNF-α), mouse interleukin-1β (IL-1β), mouse inducible NO synthase (iNOS), and GAPDH were as follows: IL-6, 5′-GGA AAT GAG AAA AGA GTT GTG CAA T-3′ (sense) and 5′-CCT TAG CCA CTC CTT CTG TGA-3′ (antisense); rat TNF-α, 5′-CAC CAC GCT CTT CTG TCT ACT G-3′ (sense) and 5′-GTA CTT GGG CAG ATT GAC CTC-3′ (antisense); rat IL-1β, 5′-GGA GAA GCT GTG GCA GCT A-3′ (sense) and 5′-GCT GAT GTA CCA GTT GGG GA-3′ (antisense); rat iNOS, 5′-AGG CTT GGG TCT TGT TAG CC-3′ (sense) and 5′-GTC TCT GGG TCC TCT GGT CA-3′(antisense); mouse TNF-α, 5′-CAC CAC GCT CTT CTG TCT ACT-3′ (sense) and 5′-GCA ATG ACT CCA AAG TAG ACC TG-3′ (antisense); mouse IL-1β, 5′-GGA GAA GCT GTG GCA GCT A-3′ (sense) and 5′-GCT GAT GTA CCA GTT GGG GA-3′ (antisense); mouse iNOS, 5′-ACG CTT GGG TCT TGT TCA CT-3′ (sense) and 5′-GTC TCT GGG TCC TCT GGT CA-3′ (antisense); and GAPDH (the loading control), 5′-TCA TTG ACC TCA ACT ACA TGG T-3′ (sense) and 5′-CTA AGC AGT TGG TGG TGC AG-3′ (antisense). PCR products were electrophoresed on 1.5% agarose gels and detected under ultraviolet light. The results of 3 independent experiments were quantified using Quantity One (Bio-rad, Hercules, CA).

Nuclear and Cytoplasm Extract Preparation

Nuclear extracts of BV2 cells (3×10^5) were prepared using Nuclear Extraction Kits (IMGENEX, San Diego, CA), and crude nuclear proteins in supernatants were stored at − 70 °C.

Whole Cell Lysate Preparation

Cells were washed twice with cold 0.01 M PBS and lysed in RIPA buffer (50 mM Tris-HCl (pH 7.4), 1% NP-40, 0.25% sodium deoxycholate, 150 mM NaCl, and complete Mini protease inhibitor cocktail tablets (Roche, Basel, Switzerland)). Lysates were centrifuged for 10 min at 15,870 × g at 4 °C and supernatants were stored at − 70 °C.

Immunoblot Analysis

Proteins (10 μg) were separated in 6 or 12% sodium dodecyl sulfate-polyacrylamide gels. After blocking with 5% nonfat milk for 1 h, membranes so obtained were incubated with primary antibodies (all diluted 1:1000) for anti-IκB-α (Santa Cruz Biotechnology, Santa Cruz, CA), anti-α-tubulin (Cell Signaling, Danvers, MA), anti-p65 (Santa Cruz Biotechnology), anti-Lamin B (Santa Cruz Biotechnology), anti-P-selectin (Santa Cruz Biotechnology), anti-ICAM-1 (Santa Cruz Biotechnology), anti-PSGL-1 (Santa Cruz Biotechnology), and anti-LFA-1 (BD Transduction Laboratories, San Jose, CA) overnight at 4 °C. The next day, blots were detected using a chemiluminescence kit (Roche, Basel, Switzerland) using HRP-conjugated secondary antibodies (1:2000; Santa Cruz Biotechnology).

Transient Transfection and the Luciferase Assay

BV2 cells (1.5×10^5) were seeded in 24-well plates containing DMEM and 1 day later transfected with a NF-κB reporter plasmid, which contained 5 copies of the NF-κB response element, which drives the transcription of the luciferase reporter gene (Promega, Madison, WI) using Lipofectamine 2000 transfection reagent (Invitrogen, Carlsbad, CA). Transfection procedures and the luciferase assay were carried out as previously described [12].

NF-κB Binding Activity Assay

DNA binding activities of p65 in nuclear extracts or of recombinant p65 were assessed using a TransAM NF-κB p65 assay kit (Active Motif, Carlsbad, CA) by following the manufacturer's recommendation.

Cell Adhesion Assay and Transendothelial Cell Migration Assay

Cell adhesion assay and transendothelial cell migration assay were carried out as previously described [16]. In brief, HUVECs were treated with DIPOPA (5 or 10 mM), DEOPA (5 or 10 mM), or EP (10 or 20 mM) for 1 h and then activated by treating them with TNF-α (10 U/ml) for 12 h before adhesion or migration assay. For the adhesion assay, dHL-60 (2×10^5) cells were added to HUVEC monolayers (1×10^5) and incubated for 30 min at 37 °C, washed twice with ice-chilled 0.01 M PBS, and fixed with 4% paraformaldehyde. Nonadherent dHL-60 cells were carefully removed and were fixed with 4% PFA and examined under a Zeiss LSM 510 META confocal microscope (Carl Zeiss, Oberkochen, Germany). Representative images were processed using a 3-D reconstruction program (AIM, Carl-Zeiss-Strasse, Oberkochen, Germany) and visualized in orthogonal views.

Statistical Analysis

2-sample comparisons were performed using the Student's *t* test and multiple comparisons by 1-way or 2-way analysis of variance (ANOVA) followed by *post hoc* testing. PRISM software 5.0 (Graph Pad Software) was used for the analysis. Results are presented as means ± SEMs and statistical difference was accepted for p values < 0.05.

Results

Neuroprotective Potencies of 3 DEOPA Derivatives in the Postischemic Brains

3 DEOPA derivatives were synthesized (Fig. 1a); they are DIPOPA (N,N-diisopropyl-2-oxopropanamide), DPOPA (N,N-dipropyl-2-oxopropanamide), and DIBOPA (N,N-diisobutyl-2-oxopropanamide), and their neuroprotective effects were compared with those of DEOPA or EP in a rat MCAO model. DIPOPA, DPOPA, DIBOPA, DEOPA, or EP were administered intravenously, at 5 mg/kg concentration at 6 h post-MCAO, and infarct volumes were assessed at 2 days after surgery. Infarct volumes were reduced in the MCAO + DPOPA, MCAO + DIBOPA, MCAO + DIPOPA, MCAO + DEOPA, and MCAO + EP groups to 89.1 ± 8.9% ($n = 5$), 73.3 ± 2.0% ($n = 4$, $p < 0.05$), 21.2 ± 6.2% ($n = 4$, $p < 0.01$), 19.3 ± 5.8% ($n = 5$, $p < 0.01$), and 45.2 ± 7.9% ($n = 4$, $p < 0.05$), respectively, *versus* that of PBS-treated MCAO controls (Fig. 1b, c). These results demonstrate that neuroprotective potency of DIPOPA was superior to those of DPOPA, DIBOPA, and EP but similar to that of DEOPA.

DIPOPA Has a Wider Therapeutic Time Window in the Postischemic Brain

To examine the neuroprotective potency of DIPOPA in more detail, 1, 2, or 5 mg/kg of DIPOPA was administered intravenously at 6 h post-MCAO. Mean infarct volumes assessed at 2 days post-MCAO were reduced to 89.4 ± 2.7% ($n = 4$), 73.0 ± 0.4% ($n = 4$, $p < 0.01$), and 21.2 ± 6.2% ($n = 4$, $p < 0.01$), respectively, *versus* PBS-treated MCAO controls, indicating DIPOPA dose-dependently suppressed infarct volume (Fig. 2a, b). Interestingly, when DIPOPA (5 mg/kg) was administered at 9 or 12 h post-MCAO, mean infarct volumes at 2 days post-MCAO reduced to 39.5 ± 6.9% ($n = 4$, $p < 0.01$) and 73.7 ± 8.0% ($n = 4$, $p < 0.05$), respectively (Fig. 2c, d). The infarct reductions obtained by 9 h postadministration of DIPOPA were significantly greater than those by DEOPA (Fig. 2c, d), indicating that the therapeutic time window of DIPOPA was wider than that of DEOPA.

Suppressions of Neurological Deficits and Motor Impairments by DIPOPA

Mean modified neurological severity scores (mNSSs) of the treatment-naïve MCAO control group was 10.5 ± 0.5 ($n = 4$) at 2 days post-MCAO. The neurological improvement by DIPOPA (5 mg/kg) was similar to that observed for DEOPA (5 mg/kg) (3.6 ± 0.9, $n = 8$, *vs* 3.7 ± 0.7, $n = 4$) when they were administered at 6 h post-MCAO. However, the improvement by DIPOPA was not significantly greater than that of DEOPA when administered at 9 h post-MCAO (5.8 ± 1.5 *vs* 8.3 ± 0.8) (Fig. 3a). When motor activities were assessed using the rota-rod at 10 or 15 rpm at 2 days post-MCAO, mean latency (time spent on the rod) in the MCAO + DIPOPA group (5 mg/kg, 6 h posttreatment) was significantly greater than that of the PBS-treated MCAO control group (Fig. 3b). Mean latencies in the MCAO + DIPOPA and MCAO + DEOPA groups were not significantly different both at 10 and 15 rpm, but these latencies were significantly greater than those of the MCAO + EP group (Fig. 3b). However, when DIPOPA or DEOPA were administered at 9 h post-MCAO, the mean latency in the MCAO + DIPOPA group was significantly greater than that of the MCAO + DEOPA group at 15 rpm (Fig. 3c). To further examine if these beneficial outcomes are maintained for a certain period of time, DIPOPA (5 mg/kg) was administered 6 h post-MCAO and mNSS and rota-rod test were assessed for 14 days. Results showed that amelioration of mNSS was detected until 6 days post-MCAO and greater latency in the rota-rod test at 15 rpm was maintained until 14 days (Fig. 3d-f). These results confirmed that DIPOPA has a wider therapeutic window. In addition, the neuroprotective effect of DIPOPA observed in Fig. 2 is accompanied with beneficial effects on neurological and motor outcomes. Changes in physiological

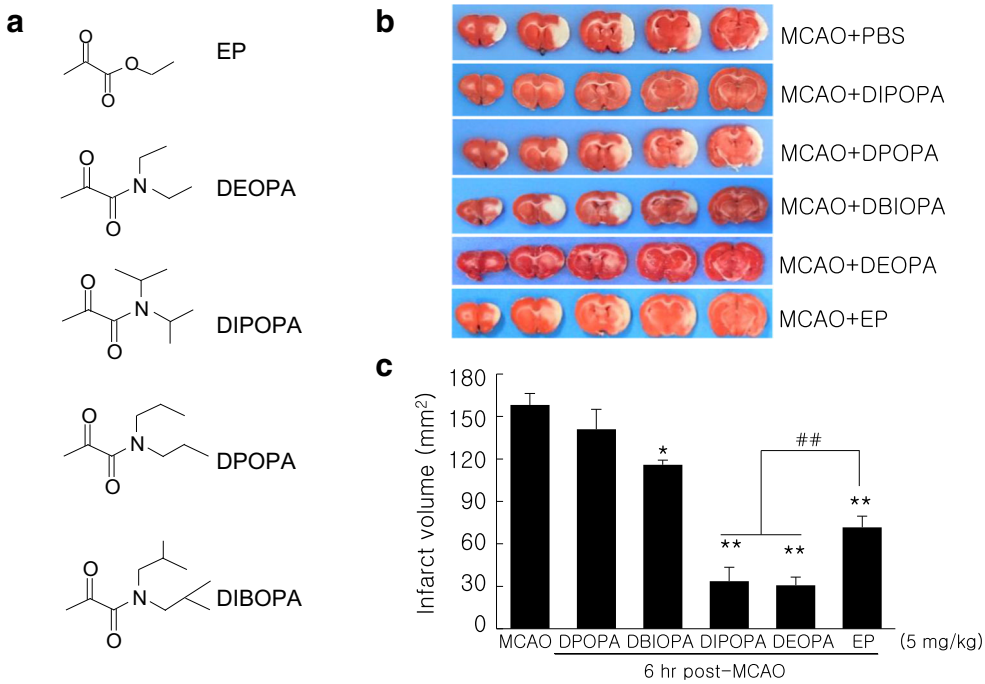

Fig. 1 Infarct suppression by the 3 DEOPA derivatives, DEOPA, and EP. (**a**) Structures of EP, DEOPA (N,N-diethyl-2-oxopropanamide), and the 3 DEOPA derivatives, namely, N,N-diisopropyl-2-oxopropanamide (DIPOPA), N,N-dipropyl-2-oxopropanamide (DPOPA), and N,N-diisobutyl-2-oxopropanamide (DIBOPA). (**b**, **c**) DIPOPA, DPOPA, DBIOPA, DEOPA, or EP was administered intravenously (5 mg/kg) at 6 h post-MCAO, and mean infarct volumes were measured at 2 days post-MCAO by TTC staining. Representative images of infarctions in coronal brain sections (**b**) and quantitative results (means ± SEMs) (**c**). MCAO, PBS-treated MCAO control animals ($n = 4$); MCAO + DIPOPA, DIPOPA-administered MCAO animals ($n = 4$); MCAO + DPOPA, DPOPA-administered MCAO animals ($n = 5$); MCAO + DBIOPA, DBIOPA-administered MCAO animals ($n = 4$); MCAO + DEOPA, DEOPA-administered MCAO animals ($n = 5$); MCAO + EP, EP-administered MCAO animals ($n = 4$). $^{*}p < 0.05$, $^{**}p < 0.01$ *versus* the MCAO group; $^{\#\#}p < 0.01$ *versus* the MCAO + EP group

variables were not detected in both normal and MCAO-subjected animals injected with DIPOPA, indicating that physiological parameters were not influenced by DIPOPA (Table 1). In addition, when we measured the rCBF using a laser Doppler flowmeter with or without DIPOPA treatment, changes in blood flow levels were not detected both in control and in MCAO (5 mg/kg, 1 h post-MCAO treatment) animals (Supplement Figure S1). Therefore, DIPOPA has no effect on the regional blood flow of the brain.

Anti-Inflammatory Effects of DIPOPA in the Postischemic Brain

We previously reported that DEOPA exhibits a robust anti-inflammatory effect in the postischemic brain [16]. Here, we examined the anti-inflammatory effects of DIPOPA and compared them with those of DEOPA. DIPOPA (5 mg/kg) was administered at 6 h post-MCAO and brain sections obtained at 2 days post-MCAO were stained with antibody against Iba-1 (a marker of cells of myeloid origin) or Mac2 (a marker of activated resident microglia). In sham controls, Iba-1^{+} cells were found throughout brain parenchyma and exhibited ramified morphology, indicative of a resting state (Fig. 4a). In contrast, in the cortices of ipsilateral hemispheres of PBS-treated MCAO controls, Iba-1^{+} cells exhibited an amoeboid form, indicating an activated state (Fig. 4b). However, Iba-1+ cells maintained the ramified form in both DIPOPA and DEOPA-treated groups (Fig. 4c, d). In contrast to Iba-1^{+} cells, Mac2^{+} cells were rarely detected in sham controls (Fig. 4f), but obvious in PBS-treated MCAO controls (Fig. 4g). However, Mac2^{+} cell numbers were significantly lower in the MCAO + DIPOPA group than in the PBS-treated MCAO controls and the suppressive effect of DIPOPA was similar to that of DEOPA (Fig. 4h-l). Moreover, as it was expected, the suppressive effects of DIPOPA and DEOPA were greater than those of EP (Fig. 4j, l). Importantly, DIPOPA suppressed proinflammatory marker (iNOS, TNF-α, Il-6, IL-1β) inductions in postischemic brain cortices more effectively than DEOPA (Fig. 4m, n). Together, these results indicate DIPOPA has robust anti-inflammatory effects and that suppressions of inflammatory cytokine induction are significantly greater than those elicited by DEOPA.

Suppression of Vascular Neutrophil Activation by DIPOPA

Next, we examined whether DIPOPA inhibits neutrophil infiltration in the postischemic brain. DIPOPA (5 mg/kg) was

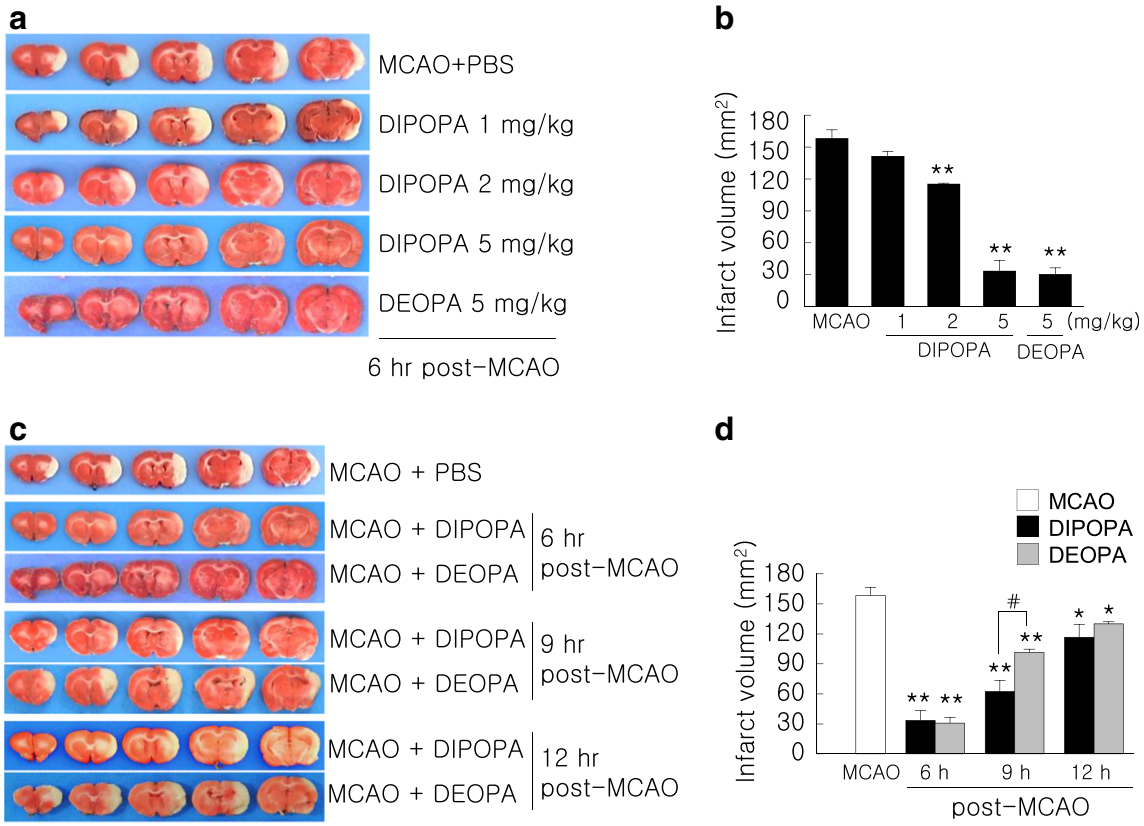

Fig. 2 Neuroprotective potency of DIPOPA. (**a**, **b**) DIPOPA (1, 2, or 5 mg/kg) or DEOPA (5 mg/kg) were administered intravenously at 6 h post-MCAO, and mean infarct volumes were measured at 2 days post-MCAO by TTC staining. (**c**, **d**) DIPOPA or DEOPA (all at 5 mg/kg) were treated intravenously at 6, 9, or 12 h post-MCAO, and mean infarct volumes were measured at 2 days post-MCAO by TTC staining. Representative images of infarctions in coronal brain sections (**a**, **c**) and quantitative results (means ± SEMs) (**b**, **d**). MCAO, PBS-treated MCAO control animals ($n = 4$); MCAO + DIPOPA, DIPOPA (1, 2, or 5 mg/kg)-administered MCAO animals ($n = 12$, $n = 4$ per group); MCAO + DEOPA, DEOPA-administered MCAO animals ($n = 5$). $*p < 0.05$, $**p < 0.01$ *versus* the MCAO group; $\#\#p < 0.01$ *versus* the MCAO + DIPOPA group

administered at 6 h post-MCAO and brain sections obtained at 12 h post-MCAO were stained with antibody against MPO (a neutrophil marker) (Fig. 5a) Similar to Mac2 staining, MPO^+ cells were rarely detected in sham controls (Fig. 5b) and significantly increased in PBS-treated MCAO controls but not in the MCAO + DIPOPA group (Fig. 5c-g). The suppressive effect of DIPOPA was greater than that of EP, but comparable to DEOPA (Fig. 5d-g). Marked suppression of MPO^+ cells in the brains of animals in the DIPOPA-administered MCAO group and the fact that DIPOPA was administered intravenously prompted us to examine whether DIPOPA suppressed neutrophil infiltration by inhibiting activation of neutrophil localized in peripheral blood. DIPOPA (5 mg/kg) was administered at 6 h post-MCAO and neutrophils were purified from peripheral blood at 12 h post-MCAO and levels of cell adhesion molecules expressed in neutrophils were examined (Fig. 5a). The protein levels of PSGL-1 and LFA-1, which are known to be involved in the transendothelial migration of neutrophils [22, 23], were induced at 12 h post-MCAO (Fig. 5h, i). However, these inductions were significantly suppressed in neutrophils prepared from the MCAO + DIPOPA group (Fig. 5h, i). Furthermore, DIPOPA suppressed these inductions more efficiently than DEOPA or EP, confirming that intravenous administration of DIPOPA effectively inhibited vascular neutrophil activation.

Suppressions of Nitrite and Proinflammatory Marker Inductions in Activated Microglia by DIPOPA

To confirm the anti-inflammatory effects of DIPOPA, BV2 cells (a microglia cell line) were treated with LPS (100 ng/ml) for 24 h and nitrite levels were measured in the presence or absence of DIPOPA. Neither DIPOPA nor DEOPA had any cytotoxic effect at 5 or 10 mM in BV2 cells, whereas EP at 10 mM exhibited slight cytotoxicity (Fig. 6a). BV2 cells pretreated with DIPOPA (1, 5, or 10 mM, 1 h) effectively suppressed LPS-induced nitrite production, and at 5 mM, DIPOPA reduced nitrite production to the basal level (Fig. 6b). Importantly, the efficacies of DIPOPA at 1 or 5 mM were

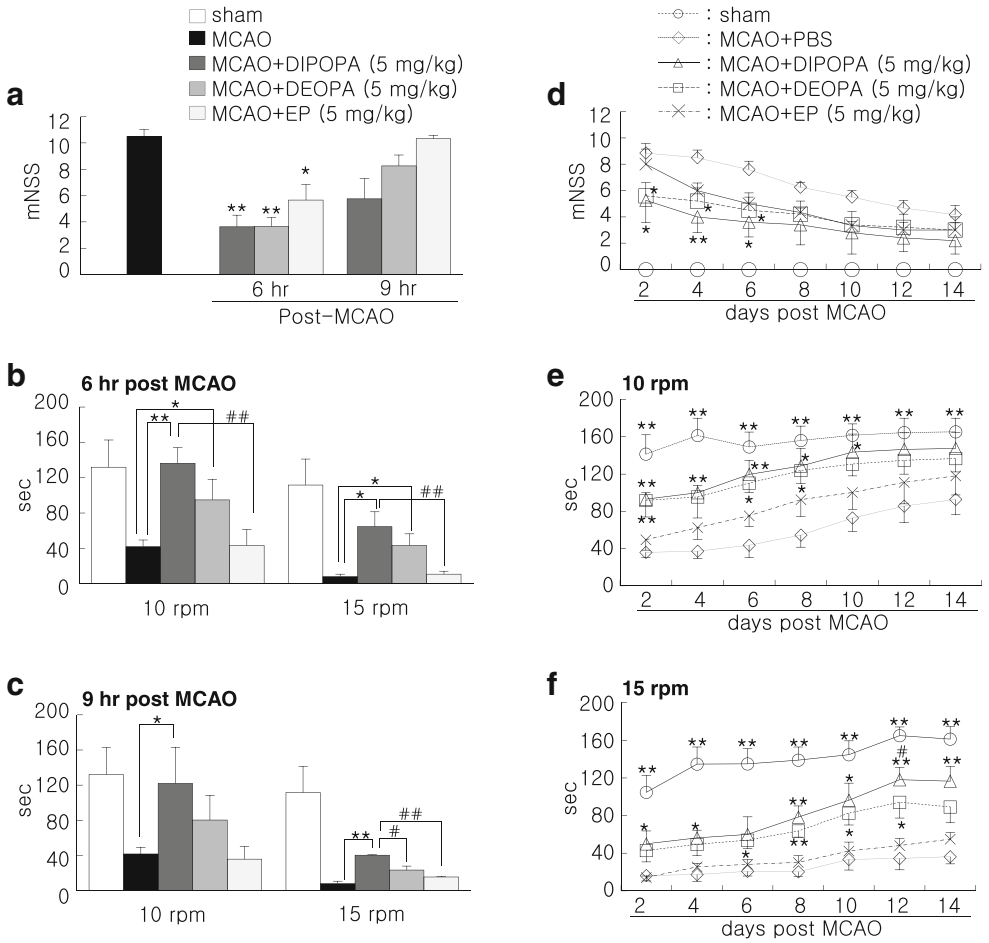

Fig. 3 Prevention of neurological and motor deficits by DIPOPA. (**a**) DIPOPA, DEOPA, or EP (5 mg/kg) was administered 6 or 9 h post-MCAO, and neurological deficits were evaluated using modified neurological severity scores at 2 days post-MCAO. (**b**, **c**) The rota-rod test was performed at 10 or 15 rpm at 2 days post-MCAO on animals (with a 1-h rest period between tests) administered DIPOPA, DEOPA, or EP (5 mg/kg) at 6 or 9 h post-MCAO. (**d**-**f**) DIPOPA, DEOPA, or EP (5 mg/kg) was administered 6 h post-MCAO, and neurological deficits were evaluated (**d**) and the rota-rod test was performed at 10 or 15 rpm (**e**, **f**) at 2, 4, 6, 8, 10, 12, or 14 days post-MCAO. Sham, sham-operated animals ($n = 8$); MCAO + PBS, PBS-treated MCAO control animals ($n = 9$); MCAO + DIPOPA, the DIPOPA-administered MCAO animals ($n = 13$); MCAO + DEOPA, the DEOPA-administered MCAO animals ($n = 9$); MCAO + EP, the EP-administered MCAO animals ($n = 9$). $*p < 0.05$, $**p < 0.01$ *versus* the MCAO group; $\#p < 0.05$, $\#\#p < 0.01$ *versus* the MCAO + DIPOPA group

greater than those of DEOPA and were greater than those of EP at all concentrations tested (Fig. 6b). Similarly, DIPOPA (1 mM) markedly suppressed LPS-induced expressions of proinflammatory markers (IL-6, iNOS, IL-1β, and TNF-α), and again, the efficacy of DIPOPA was significantly greater than those of DEOPA or of EP (Fig. 6c-f).

Table 1 Physiological parameters after treatment of DIPOPA, DEOPA, or EP

	Base ($n = 5$)				During ischemia ($n = 5$)			
	Vehicle	DIPOPA	DEOPA	EP	Vehicle	DIPOPA	DEOPA	EP
Rectal temperature, °C	37.1 ± 0.1	37.2 ± 0.4	37.2 ± 0.1	37.4 ± 0.3	38.0 ± 0.1	37.6 ± 0.0	37.8 ± 0.1	37.7 ± 0.0
pH	7.6 ± 0.0	7.5 ± 0.1	7.6 ± 0.1	7.5 ± 0.1	7.6 ± 0.0	7.6 ± 0.0	7.6 ± 0.0	7.6 ± 0.0
pCO_2, mmHg	28.5 ± 1.0	24.5 ± 0.7	22.8 ± 1.5	25.8 ± 0.3	25.0 ± 0.9	25.2 ± 0.2	26.9 ± 0.2	23.8 ± 0.2
pO_2, mmHg	144.3 ± 4.3	134.3 ± 9.8	120.3 ± 6.7	136.0 ± 6.4	128.8 ± 4.4	137.5 ± 3.2	134.7 ± 3.5	125.5 ± 1.8
Glocuse, mg/dl	107.3 ± 3.1	113.5 ± 10.1	115.0 ± 1.7	91.3 ± 2.0	96.4 ± 1.9	98.2 ± 1.7	96.3 ± 1.7	95.8 ± 2.2

Values are means ± SD ($n = 5$). 1-way analysis of variance revealed no significant intergroup difference for any variance

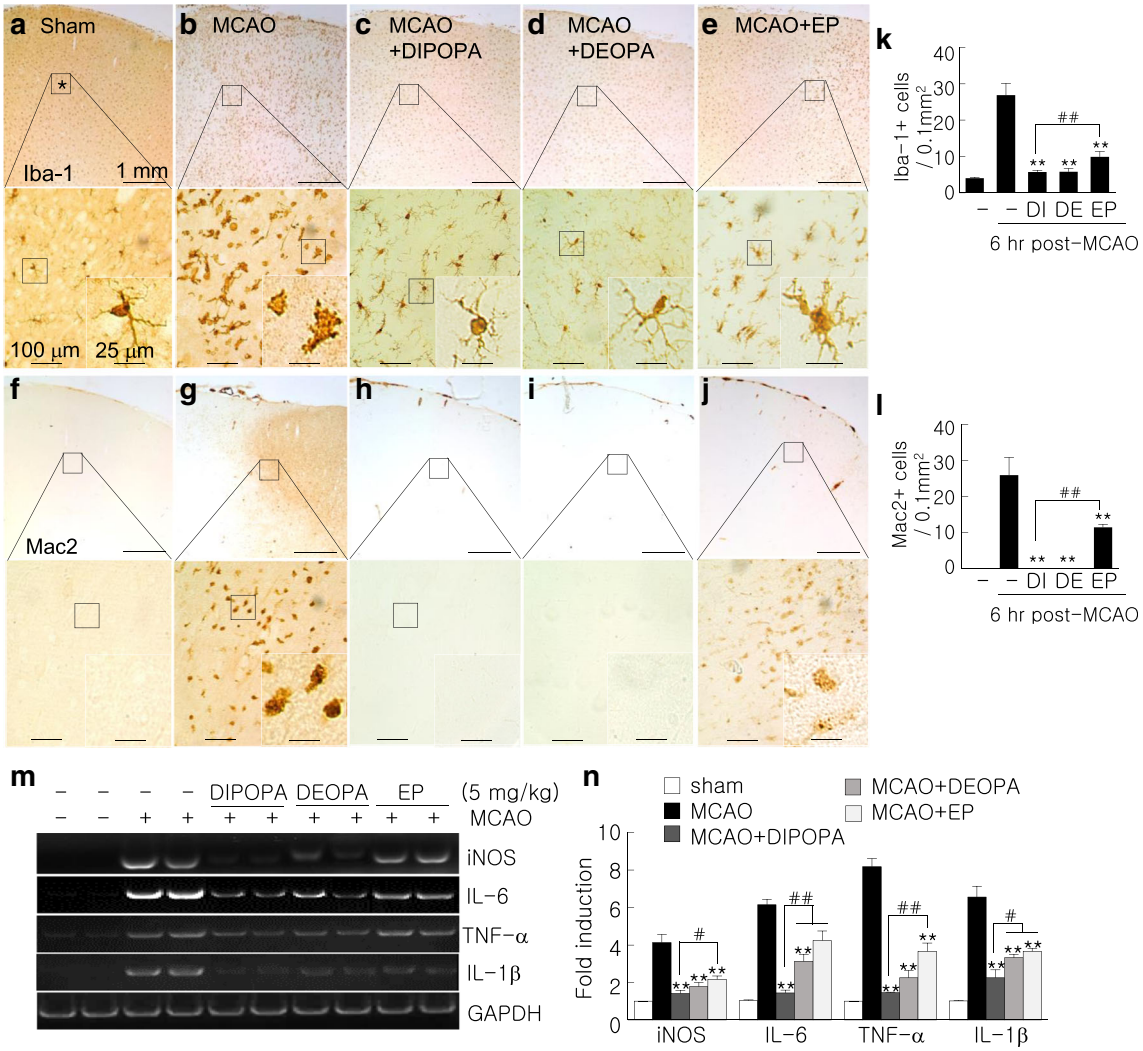

Fig. 4 Suppression of inflammatory processes by DEOPA in the postischemic brain. DIPOPA, DEOPA, or EP (5 mg/kg) was administered 6 h post-MCAO, and immunohistochemistry (**a**-**l**) and RT-PCR (**m**-**n**) were carried out at 2 days post-MCAO. (**a**-**j**) Coronal brain sections were obtained 2 days after surgery in the sham (**a**, **f**), MCAO (**b**, **g**), MCAO + DIPOPA (**c**, **h**), MCAO + DEOPA (**d**, **i**), and MCAO + EP (**e**, **j**) groups and stained using anti-Iba-1 (**a**-**e**) or anti-Mac2 (**f**-**j**) antibodies. The images in the lower boxes (**a**-**j**) are high-magnification photographs, and insets in each image are high-magnification photographs of the indicated regions (white box). Photographs are representative of 3 independent experiments. Scale bars in **a**-**j** represent 1 mm and those in high-magnification photographs represent 100 μm or 25 μm. (**k**-**l**) Numbers of Iba-1$^+$ and Mac2$^+$ cells in indicated regions in a (*, 0.1 mm^2) were counted and are presented as means ± SEMs ($n = 12$ from 3 animals). (**m**-**n**) RT-PCR samples were prepared from the indicated region (the black box) at 2 days post-MCAO and RNA levels of iNOS, IL-6, TNF-α, and IL-1β are presented as means ± SEMs ($n = 3$). Sham, sham-operated controls ($n = 6$); MCAO + PBS, PBS-treated MCAO control rats ($n = 6$); MCAO + DIPOPA, DIPOPA-administered MCAO rats ($n = 6$); MCAO + DEOPA, DEOPA-administered MCAO rats ($n = 6$); MCAO + EP, EP-administered MCAO rats ($n = 6$). $^{**}p < 0.01$ *versus* the MCAO group; $\#p < 0.05$, $\#\#p < 0.01$ *versus* the MCAO + DIPOPA group

Blockade of Neutrophil–Endothelial Adhesion and of Transendothelial Neutrophil Migration by DEOPA

Neutrophil–endothelial cell cocultures were used to examine suppressive effects of DIPOPA on neutrophil–endothelial interactions and on the expressions of genes involved in these processes. Prior to coculture, HUVECs and differentiated human promyelocytic leukemia cells (dHL60 cells) were activated by treating them with TNF-α (10 U/ml) for 12 h (Fig. 7a). The protein expressions of adhesion molecules in activated HUVECs (ICAM-1 and p-selectin) and dHL60 cells (LFA-1 and PSGL-1) were significantly increased by TNF-α (Fig. 7b, c). However, when HUVECs and dHL60 cells were pretreated with DIPOPA or DEOPA (10 mM, 1 h) before being treated with TNF-α, these increases were significantly reduced and DIPOPA had a significantly greater effect than DEOPA or EP (Fig. 7b, c). After activation, dHL60 cell-to-HUVEC monolayer attachment was 15-fold higher than for TNF-α-untreated cells (Fig. 7d, e) and pretreatment with DIPOPA (10 mM) prior

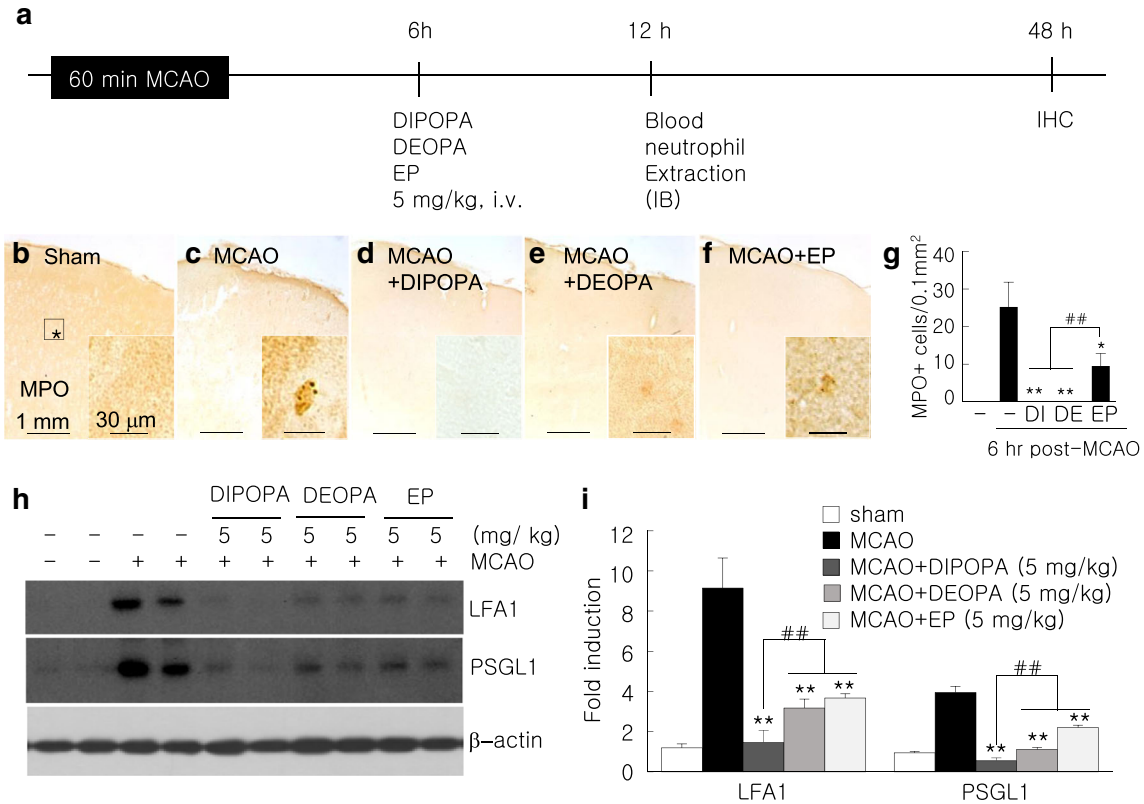

Fig. 5 Suppression of vascular neutrophil activation after MCAO by DIPOPA. (**a**) DIPOPA, DEOPA, or EP (5 mg/kg) was administered 6 h post-MCAO, and neutrophils were purified from peripheral blood for immunoblot analysis at 12 h post-MCAO and immunohistochemistry was carried out at 48 h post-MCAO. (**b**-**g**) Coronal brain sections were obtained 48 h after surgery from the sham (**b**), MCAO (**c**), MCAO + DIPOPA (**d**), MCAO + DEOPA (**e**), and MCAO + EP (**f**) groups. Neutrophils were stained using anti-MPO antibody, and insets are high-magnification photographs of the indicated regions (*) in **b**. Photographs are representative of 3 independent experiments. Scale bars in **a**-**f** represent 1 mm and those in insets represent 50 μm. (**g**) Numbers of MPO^+ cells in indicated regions in **b** (*, 0.1 mm^2) were counted and are presented as means ± SEMs ($n = 12$ from 3 animals). (**h**-**i**) Vascular neutrophils were extracted from blood samples at 12 h post MCAO, and the expressions of PSGL-1 and LFA-1 in neutrophils were measured by western blot. Representative immunoblots and protein levels presented as means ± SEMs ($n = 3$). Sham, sham-operated rats ($n = 5$); MCAO + PBS, PBS-treated MCAO control rats ($n = 5$); MCAO + DIPOPA, DIPOPA-administered MCAO rats ($n = 5$); MCAO + DEOPA, DEOPA-administered MCAO rats ($n = 5$); MCAO + EP, EP-administered MCAO rats ($n = 5$). $^{**}p < 0.01$ *versus* the MCAO group; $\#p < 0.05$, $\#\#$ $p < 0.01$ *versus* the MCAO + DIPOPA group

to TNF-α treatment significantly reduced cell to monolayer attachment (Fig. 7d, e). Pretreatment with DEOPA (10 mM) or EP (10 mM) also reduced cell-to-monolayer attachment but to lesser extents (Fig. 7d, e). Similarly, numbers of dHL60 cells that migrated through HUVEC monolayers were markedly reduced by pretreating both cell types with DIPOPA (10 mM) and these reductions were also greater than those observed for DEOPA or EP (Fig. 7f, g). These results indicate DIPOPA inhibited neutrophil/endothelial cell interactions and the transendothelial migration of neutrophils, at least in part, by repressing the inductions of cell adhesion molecules.

Suppression of NF-κB Activity by DIPOPA Via the Inhibitions of IκB-α Degradation in Cytosol and of p65 to DNA Binding in the Nucleus

Observations of the marked anti-inflammatory effects of DIPOPA *in vivo* and *in vitro* prompted us to examine the effects of DIPOPA on the NF-κB signaling pathway. The amount of IκB-α in the cytoplasm of LPS-treated BV2 cells was significantly reduced by LPS treatment (100 ng/ml, 15 min), and this decrease was dramatically suppressed by pretreating DIPOPA (5 mM, 1 h) (Fig. 8a, b). Nuclear translocation of p65 was also markedly suppressed by DIPOPA (Fig. 8c, d). However, levels of α-tubulin and lamin B were unchanged in cytoplasm and nuclei, respectively, when cells were pretreated with DIPOPA (Fig. 8a, c). These results suggest DIPOPA suppressed the nuclear translocation of p65 probably by inhibiting IκB-α degradation in cytosol, and importantly, the effects of DIPOPA were greater than those of EP or DEOPA (Fig. 8a-d). When we measured LPS-induced NF-κB activity using NF-κB-Luc reporter plasmid containing 5 copies of the NF-κB consensus sequence (GGGAATTTCC), pretreatment with DIPOPA (5 mM) suppressed NF-κB activity to 50.5 ± 8.4% ($n = 4$) of that of LPS-induced BV2 cells, and this suppression was greater than those obtained by pretreating cells with the same

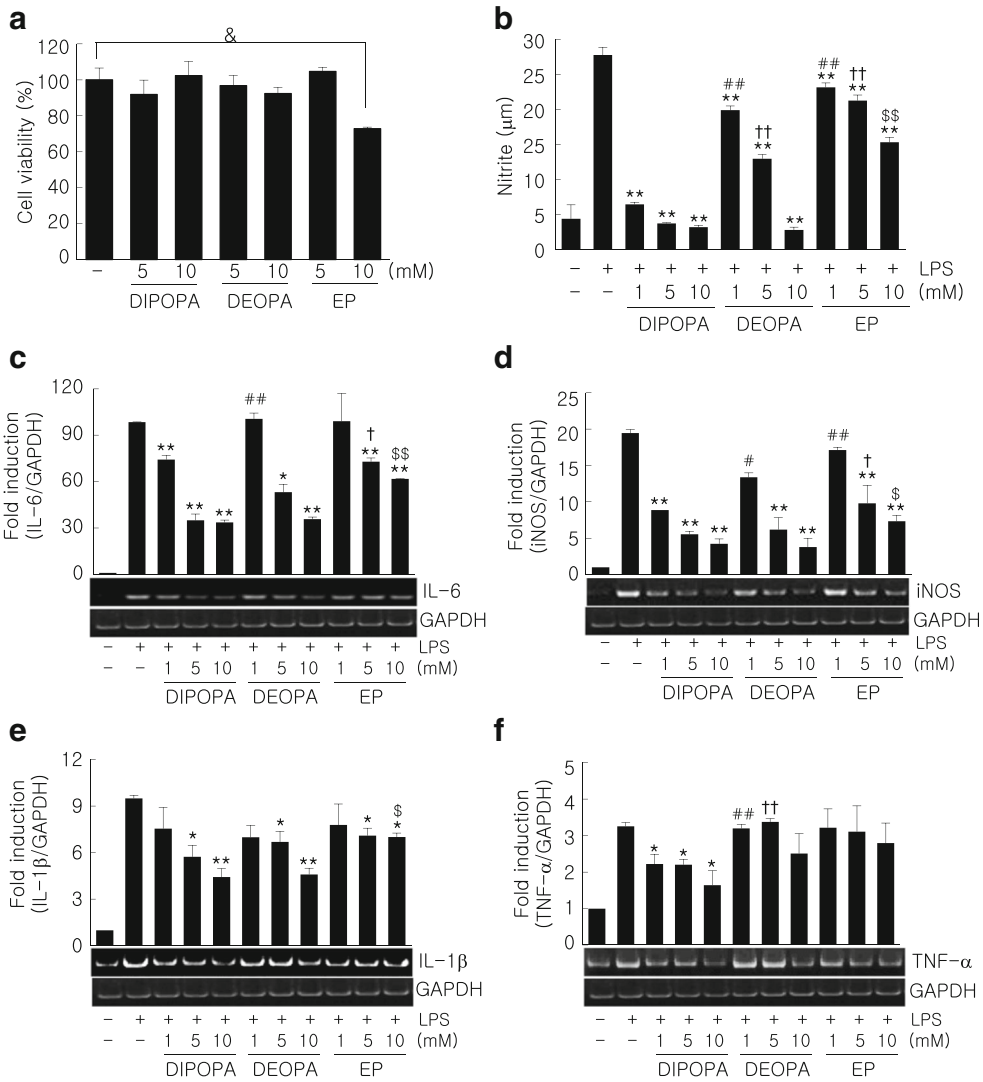

Fig. 6 Suppression of the LPS-induced activation of BV2 cells by DIPOPA. (**a**) The cytotoxicities of DIPOPA, DEOPA, and EP were measured by cell viability assay using CCK-8. (**b**-**f**) Nitrite production (**b**) and expressions of proinflammatory markers (**c**-**f**) were assessed using a Griess assay and by RT-PCR, respectively. BV2 cells (0.7×10^4 cells/well in 24-well culture dishes) were pretreated with DIPOPA, DEOPA, or EP (1, 5, or 10 mM) for 1 h, washed, and then incubated with LPS (100 ng/ml) for 24 h. Changes in nitrite and proinflammatory cytokine mRNA levels are presented as means ± SEMs. &$p < 0.05$ *versus* vehicle controls; *$p < 0.05$, **$p < 0.01$ *versus* LPS treatment alone; #$p < 0.05$, ##$p < 0.01$ *versus* 1 mM of DIPOPA-treated cells; †$p < 0.05$, ††$p < 0.01$ *versus* 5 mM of DIPOPA-treated cells; \$$p < 0.05$, \$\$$p < 0.01$ *versus* 10 mM of DIPOPA-treated cells

concentration of DEOPA (62.6 ± 1.0%, $n = 4$) (Fig. 8e). In addition, the DNA binding activity of p65 induced by LPS was suppressed by DIPOPA more so than by DEOPA (Fig. 8f). Together, these results indicate that the anti-inflammatory effect of DIPOPA is due to its suppression of NF-kB activity and that its effect is significantly greater than those of DEOPA or EP.

Discussion

Ethyl pyruvate has been reported to exert robust protective effects due to its anti-oxidative, anti-inflammatory, anti-apoptotic, and direct ion-chelating effects [8, 13, 24–27], and thus, many investigators have tried to develop new EP derivatives harboring additional advantages in addition to its known pharmacological effects. In the present study, we reported DIPOPA, in which the diethylamino group of DEOPA [16] was substituted with a diisopropylamino group, showed greater neuroprotective and anti-inflammatory effects than EP or DEOPA. Although the neuroprotective effects of DIPOPA in the postischemic brain were comparable to those of DEOPA, it was found to have a wider therapeutic window than DEOPA *in vivo* and its overall anti-inflammatory effects were superior to those of DEOPA or EP.

In a previous study, we synthesized EP isosters by substituting the ethoxy group of EP with thioester (S-ethyl-2-oxopropanamide, EOP), N-propyl (EOPA), or diethylamine (N,N-diethyl-2-oxopropanamide, DEOPA) groups. We found all 3 isosters have infarct-suppressing effects in our MCAO stroke model in the order of DEOPA → EOPA → EP → EOP, and attributed the robust neuroprotective effect of DEOPA to its anti-inflammatory effects and anti-excitotoxic effects [16]. In the present study, DIPOPA, in which the diethylamino group of DEOPA was substituted with a diisopropylamino group, was observed to exert significantly greater anti-inflammatory effects than DEOPA *in vivo* and *in vitro* (Figs. 4, 5, 6, and 7). Like in DEOPA, substitutions in all 3 derivatives tested in the present study harbor symmetrical structures (Fig. 1a). DIPOPA is less

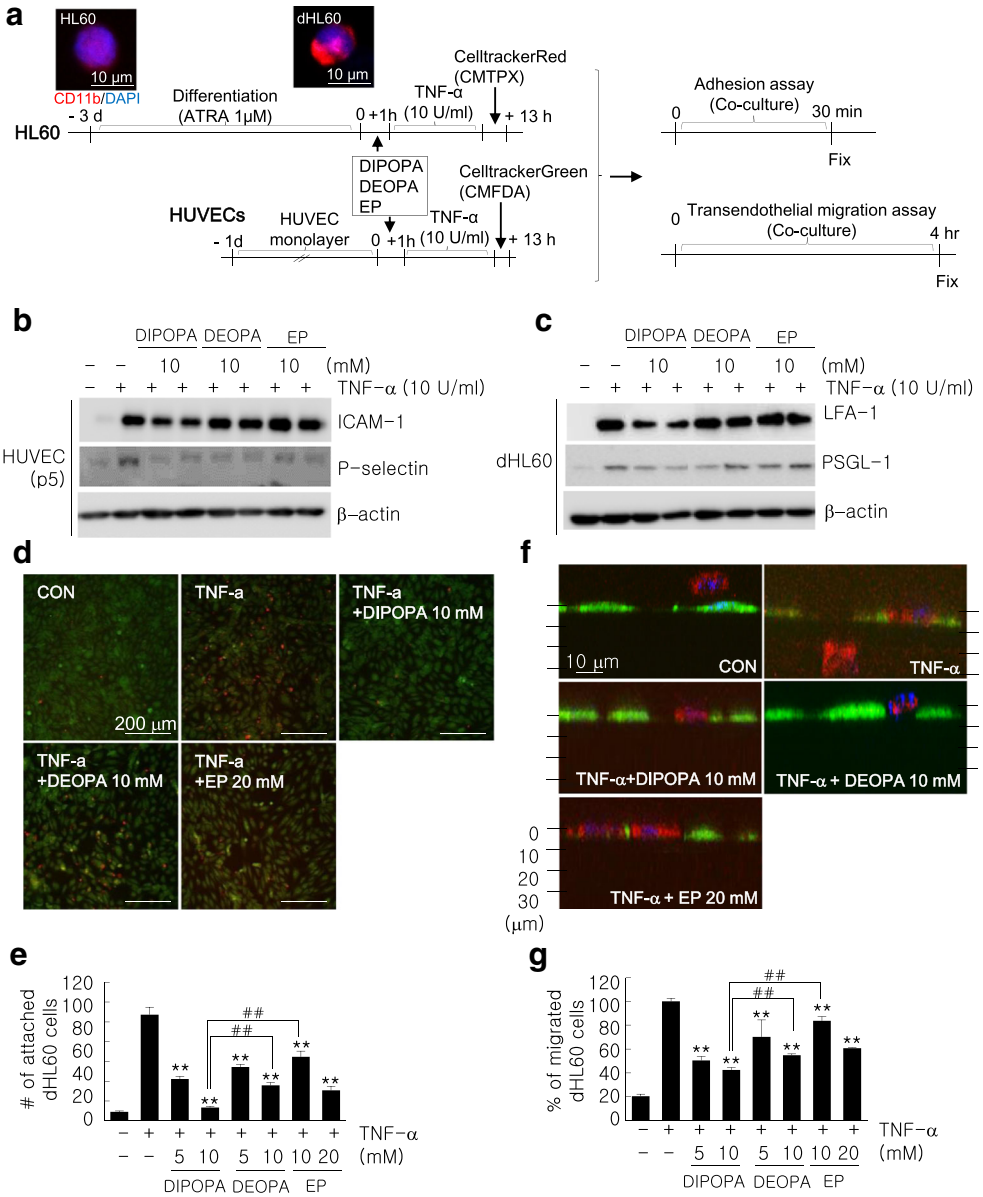

Fig. 7 Suppressions of neutrophil to endothelial adhesion, transendothelial neutrophil migration, and chemokine and cell adhesion molecule inductions by DIPOPA. (**a**) HL-60 cells were activated by 1 μM of ATRA for 3 days, and HUVEC cells were plated on gelatin-coated plates 1 day before assays. Both cell types were treated with DIPOPA, DEOPA, or EP for 1 h and activated with TNF-α (10 U/ml) for 12 h. HL-60 cells and HUVECs were labeled with CellTracker™ Red CMFDA or CellTracker Green CMTPX Dye, respectively. (**b**, **c**) After TNF-α treatment, adhesion molecule expressions were determined in both cell lines by western blot and beta-actin was used as the loading control. (**d**, **e**) For the adhesion assay, HL-60 cells and HUVECs were cocultured for 30 min, washed with chilled PBS 3 times, fixed, and the numbers of attached dHL-60 cells were counted. (**f**, **g**) Labeled dHL-60 cells were seeded on HUVEC monolayers in upper Boyden chambers, cocultured for 4 h, and fixed. Numbers of dHL-60 cells that measured were determined using a MTT assay, and results are presented as means ± SEMs ($n = 3$). Scale bars in **d** and **f** represent 200 μm or 10 μm. $^{**}p < 0.01$ *versus* TNF-α-treated control cells; $^{\#\#}p < 0.01$ *versus* 10 mM of DIPOPA-treated group

bulky compared to DIBOPA; however, it is more bulky and might exhibit a stronger steric effect compared to DEOPA and DPOPA, since it contains a secondary amine (Fig. 1a). It is interesting to mention that, when Cordopatis et al. [28] compared the binding activities of analogues of angiotensin II, which contain alkyl substitution on the side chain of the aspartic acid residue in position 1, the dipropyl analogue showed better activity than the diisopropyl analogue. Therefore, the effects of different alkyl substitutions seemed to be context-dependent and the molecular mechanism underlying enhanced anti-inflammatory and anti-excitotoxic effects exerted by diisopropyl substitution in DIPOPA need further investigation.

Microglia and neutrophils play major roles in the evocation of inflammatory processes during the acute phase of stroke and exacerbate ischemic damage [29]. Microglia, resident macrophages in the CNS, are known to be activated by DAMPs, such as, nucleotides (ATP, UTP) and HMGB1, glutamate, and ROS, which are released by damaged cells during the early stage after ischemic stroke and induce inflammation by upregulating pro-inflammatory cytokines or NO [30]. We observed DIPOPA effectively suppressed microglia activation and inflammatory cytokine induction both *in vivo* and *in vitro*, and that its potency was greater than that of DEOPA. Neutrophils are the first immune cell type to infiltrate ischemic regions after stroke and do so using cell adhesion molecules or inflammatory cytokines, and thus, aggravating inflammatory responses [31, 32]. In the present study, DIPOPA effectively inhibited neutrophil infiltration in our MCAO model and the transendothelial migration of neutrophils in our neutrophil–endothelial cell coculture system. Intriguingly, the expressions of adhesion molecules were markedly suppressed not only in brain parenchyma but in circulating neutrophils of MCAO animals. Since DIPOPA was

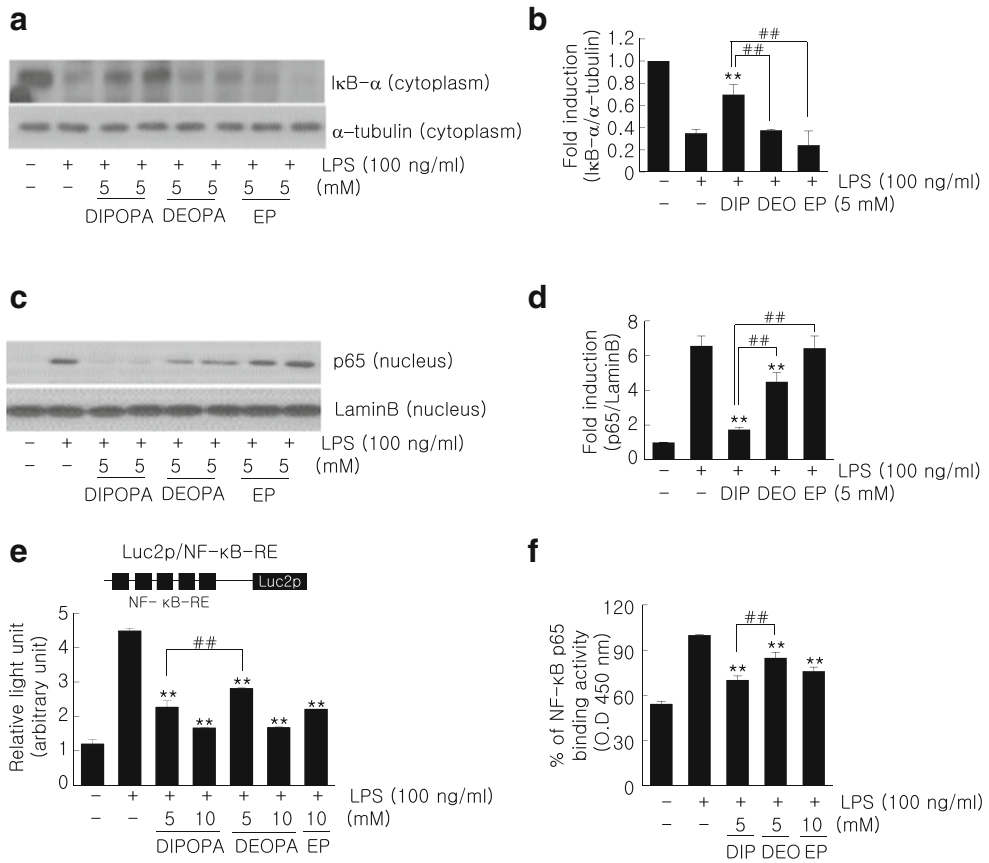

Fig. 8 Suppression of NF-kB activity by DIPOPA in LPS-treated BV2 cells. (**a**-**d**) Effects of DIPOPA, DEOPA, or EP (all at 5 mM) on cytoplasmic IκB levels (**a**, **b**) and on nuclear p65 levels (**c**, **d**) in BV2 cells were examined by immunoblotting after treating cells with LPS (100 ng/ml) for 15 min or 1 h, respectively. Alpha-Tubulin and lamin B were used as loading controls. (**e**) BV2 cells were transfected with NF-κB-Luc reporter plasmid 1 day before assay, and NF-κB activities induced by LPS (100 ng/ml) in the presence or absence of DIPOPA, DEOPA, or of EP (5 or 10 mM) were examined. NF-κB activities are presented as means ± SEMs ($n = 3$). (**f**) Endogenous NF-κB binding was assessed using the TransAM p65 assay kit in the presence or absence of DIPOPA, DEOPA, or EP (all at 5 mM). *$p < 0.05$, **$p < 0.01$ *versus* LPS treatment alone; ##$p < 0.01$ *versus* DIPOPA-treated cells

administered intravenously at 6 h post-MCAO and blood neutrophils were purified 6 h after the DIPOPA administration (Fig. 5a), significant suppressions of cell adhesion molecule induction in peripheral neutrophils were surprising, and we believe it might be a direct effect of DIPOPA on neutrophils in blood. In addition, it is notable here that anti-inflammatory effects of DIPOPA in microglia and neutrophils were markedly greater at lower dose, for example, at 1 μM. Since it has been reported that the lipophilicity of a drug is related to its efficacy [14, 33] and the ClogP values of DIPOPA and DEOPA are 0.66 and 0.126, respectively, it might be that the higher lipophilicity of DIPOPA enhances its cell permeability and its beneficial effect.

We also found that suppression of NF-kB activity underlies the anti-inflammatory effect of DIPOPA. Suppressions of IκB degradation in cytosol and subsequent nuclear translocation of p65 by DIPOPA were significantly greater than those of DEOPA (Figs. 8a-d); however, the suppression of NF-kB activity by DIPOPA at 5 mM examined by luciferase assay (Fig. 8e) did not seem greater enough compared to DEOPA, although it is statistically significant. It might be explained, at least in part, by a moderate suppressive effect of DIPOPA on NF-κB-DNA binding (Fig. 8f). Considering strong anti-inflammatory effects of DIPOPA observed *in vivo* and *in vitro*, it might be attributable to the suppressions of various steps of NF-kB activation plus additional mechanisms, which deserve further study.

Interestingly, DIPOPA and DEOPA did not inhibit HMGB1 release in LPS-treated microglia (Supplement Fig. 2), whereas EP is well known to inhibit HMGB1 release under inflammatory conditions and has been used as a specific inhibitor of HMGB1 release [2, 8, 10, 11, 34]. In addition, the anti-excitotoxic and anti-Zn^{2+} toxicity effects of DIPOPA and DEOPA were weaker than those of EP (supplement Fig. 3). Since these anti-excitotoxic and anti-Zn^{2+}-toxic effects are due to pyruvate formed during the metabolism of EP [35], we believe that these differences suggest DIPOPA and DEOPA are not metabolized to pyruvate. We suggest the differential pharmacological properties of DIPOPA, DEOPA, and EP should be studied further with respect to the difference in their molecular structure, physical properties, and metabolic processes.

Regarding the greater anti-inflammatory potency of DIPOPA than DEOPA or EP, we believe that DIPOPA might employ unknown additional molecular mechanism(s). We suggest a follow-up study be conducted to evaluate the therapeutic efficacy of DIPOPA in stroke and as a treatment of inflammation-related diseases.

Acknowledgments This work was financed by Translational Research Grant (HI17C0342) funded by Korea Health Industry Development Institute (KHIDI) (to J.-K.L.) and Medical Research Center Grant (2014R1A5A2009392) funded by the National Research Foundation (NRF) of Korea (to J.-K.L.).

Compliance with Ethical Standards

All animal studies were carried out in strict accordance with the Guide for the Care and Use of Laboratory Animals published by the National Institutes of Health (NIH, USA 2013) and complied with ARRIVE guidelines (http://www.nc3rs.org/ARRIVE). The animal protocol used in this study was reviewed and approved beforehand by the INHA University-Institutional Animal Care and Use Committee (INHA-IACUC) with respect to ethicality (Approval Number INHA-140522-297).

Publisher's note Springer Nature remains neutral with regard to jurisdictional claims in published maps and institutional affiliations.

References

1. Venkataraman R, Kellum JA, Song M, Fink MP. Resuscitation with Ringer's ethyl pyruvate solution prolongs survival and modulates plasma cytokine and nitrite/nitrate concentrations in a rat model of lipopolysaccharide-induced shock. Shock 2002;18:507–512.
2. Ulloa L, Ochani M, Yang H, et al. Ethyl pyruvate prevents lethality in mice with established lethal sepsis and systemic inflammation. Proc Natl Acad Sci USA 2002; 99: 12351–12356.
3. Yang R, Uchiyama T, Alber SM, et al. Ethyl pyruvate ameliorates distant organ injury in a murine model of acute necrotizing pancreatitis. Crit Care Med 2004; 32: 1453–1459.
4. Yu YM, Kim JB, Lee KW, Kim SY, Han PL, Lee JK. Inhibition of the cerebral ischemic injury by ethyl pyruvate with a wide therapeutic window. Stroke 2005; 36: 2238–2243.
5. Varma SD, Devamanoharan PS, Ali AH. Prevention of intracellular oxidative stress to lens by pyruvate and its ester. Free Radic Res 1998; 28: 131–135.
6. Fink MP. Ethyl pyruvate: a novel anti-inflammatory agent. Cri Care Med 2003; 31(1 Suppl): S51–56.
7. Tsung A, Kaizu T, Nakao A, et al. Ethyl pyruvate ameliorates liver ischemia-reperfusion injury by decreasing hepatic necrosis and apoptosis. Transplantation 2005; 79: 196–204.
8. Shin JH, Kim ID, Kim SW, et al. Ethyl pyruvate inhibits HMGB1 phosphorylation and release by chelating calcium. Mol Med 2015; 20: 649–657.
9. Han Y, Englert JA, Yang R, Delude RL, Fink MP. Ethyl pyruvate inhibits nuclear factor-kappaB-dependent signaling by directly targeting p65. J Pharmacol Exp Ther 2005; 312: 1097–1105.
10. Davé SH, Tilstra JS, Matsuoka K, et al. Ethyl pyruvate decreases HMGB1 release and ameliorates murine colitis. J Leukoc Biol 2009; 86: 633–643.
11. Shin JH, Lee HK, Lee HB, Jin Y, Lee JK. Ethyl pyruvate inhibits HMGB1 phosphorylation and secretion in activated microglia and in the postischemic brain. Neurosci Lett 2014; 558: 159–163.
12. Kim SW, Lee HK, Shin JH, Lee JK. Up-down regulation of HO-1 and iNOS gene expressions by ethyl pyruvate via recruiting p300 to Nrf2 and depriving It from p65. Free Radic Biol Med 2013; 65: 468–476.
13. Kim SW, Lee HK, Kim HJ, Yoon SH, Lee JK. Neuroprotective effect of ethyl pyruvate against Zn(2+) toxicity via NAD replenishment and direct Zn(2+) chelation. Neuropharmacology 2016; 5: 411–419.
14. Sappington PL, Cruz RJ Jr, Harada T, et al. The ethyl pyruvate analogues, diethyl oxaloproprionate, 2-acetamidoacrylate, and methyl-2-acetamidoacrylate, exhibit anti-inflammatory properties in vivo and/or in vitro. Biochem Pharmacol 2005; 70: 1579–1592.
15. Min S, More SV, Park JY, Jeon SB, et al. EOP, a newly synthesized ethyl pyruvate derivative, attenuates the production of inflammatory mediators via p38, ERK and NF-κB pathways in lipopolysaccharide-activated BV-2 microglial cells. Molecules 2014; 19: 19361–19375.
16. Lee HK, Kim ID, Kim SW, et al. Anti-inflammatory and anti-excitoxic effects of diethyl oxopropanamide, an ethyl pyruvate bioisoster, exert robust neuroprotective effects in the postischemic brain. Sci Rep 2017; 7: 42891.
17. Kim JB, Piao CS, Lee KW, et al. Delayed genomic responses to transient middle cerebral artery occlusion in the rat. J Neurochem 2004; 89: 1271–1282.
18. Swanson RA, Morton MT, Tsao-Wu G, Savalos RA, Davidson C, Sharp FR. A semiautomated method for measuring brain infarct volume. J Cereb Blood Flow Metab. 1990; 10: 290–293.
19. Chen J, Sanberg PR, Li Y, et al. Intravenous administration of human umbilical cord blood reduces behavioral deficits after stroke in rats. Stroke 2001; 32: 2682–2688.
20. Kim JB, Lim CM, Yu YM, Lee JK. Induction and subcellular localization of high-mobility group box-1 (HMGB1) in the postischemic rat brain. J Neurosci Res 2008; 86: 1125–1131.
21. Nash GB. Adhesion between platelets and leukocytes or endothelial cells. Methods Mol Biol. 2004; 272: 199–213.
22. Sako D, Chang XJ, Barone KM, et al. Expression cloning of a functional glycoprotein ligand for P-selectin. Cell 1993; 75: 1179–1186.
23. Ding ZM, Babensee JE, Simon SI, et al. Relative contribution of LFA-1 and Mac-1 to neutrophil adhesion and migration. J Immunol 1999; 163: 5029–5038.
24. Kim JB, Yu YM, Kim SW, Lee JK. Anti-inflammatory mechanism is involved in ethyl pyruvate-mediated efficacious neuroprotection in the postischemic brain. Brain Res 2005; 1060: 188–192.
25. Kładna A, Marchlewicz M, Piechowska T, Kruk I, Aboul-Enein HY. Reactivity of pyruvic acid and its derivatives towards reactive oxygen species. Luminescence 2015; 30: 1153–1158.
26. Song M, Kellum JA, Kaldas H, Fink MP. Evidence that glutathione depletion is a mechanism responsible for the anti-inflammatory effects of ethyl pyruvate in cultured lipopolysaccharide-stimulated RAW 264.7 cells. J Pharmacol Exp Ther 2004; 308: 307–316.
27. Wang LZ, Sun WC, Zhu XZ. Ethyl pyruvate protects PC12 cells from dopamine-induced apoptosis. Eur J Pharmacol 2005; 508: 57–68.
28. Cordopatis P, Theodoropoulos D, Guillemette G, Escher E. Studies on position 1 of angiotensin II: effects on affinity and duration of action from alkyl amide substitution. J Med Chem 1981; 24: 209–211.
29. Benakis C, Garcia-Bonilla L, Iadecola C, Anrather J. The role of microglia and myeloid immune cells in acute cerebral ischemia. Front Cell Neurosci 2015; 8: 461.

30. Iadecola C, Anrather J. Stroke research at a crossroad: asking the brain for directions. Nat Neurosci 2011; 14: 1363–1368.
31. Pinsky DJ, Naka Y, Liao H, et al. Hypoxia-induced exocytosis of endothelial cell Weibel-Palade bodies. A mechanism for rapid neutrophil recruitment after cardiac preservation. J Clin Invest 1996; 97: 493–500.
32. Yilmaz G, Granger DN. Leukocyte recruitment and ischemic brain injury. Neuromolecular Med 2010; 12: 93–204.
33. Cruz RJ Jr, Harada T, Sasatomi E, Fink MP. Effects of ethyl pyruvate and other α-keto carboxylic acid derivatives in a rat model of multivisceral ischemia and reperfusion. J Surg Res 2011; 165: 151–157.
34. Marsh JM, Williams-Karnesky RL, Stenzel-Poore MP. Toll-Like Receptor Signaling in Endogenous Neuroprotection and Stroke. Neuroscience 2009; 158: 1007–1020.
35. Zeng J, Liu J, Yang GY, Kelly MJ, James TL, Litt L. Exogenous ethyl pyruvate versus pyruvate during metabolic recovery after oxidative stress in neonatal rat cerebrocortical slices. Anesthesiology 2007; 107: 630–640.